JOC The Journal of Organic Chemistry

Article

pubs.acs.org/joc

Synthetic Precursors for $TCNQF_4^{2-}$ Compounds: Synthesis, Characterization, and Electrochemical Studies of $(Pr_4N)_2TCNQF_4$ and Li_2TCNQF_4

Jinzhen Lu,[†] Thanh Hai Le,[†] Daouda A. K. Traore,[‡] Matthew Wilce,[‡] Alan M. Bond,*[,†] and Lisandra L. Martin*[,†]

[†]School of Chemistry, Monash University, Wellington Road, Clayton, Victoria 3800, Australia

[‡]Department of Biochemistry and Molecular Biology, Monash University, Wellington Road, Clayton, Victoria 3800, Australia

Supporting Information

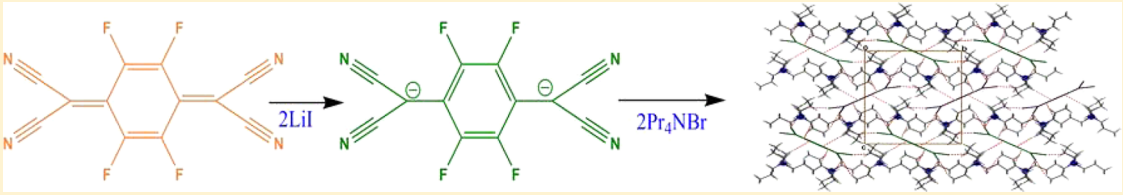

ABSTRACT: Careful control of the reaction stoichiometry and conditions enables the synthesis of both $LiTCNQF_4$ and Li_2TCNQF_4 to be achieved. Reaction of LiI with $TCNQF_4$, in a 4:1 molar ratio, in boiling acetonitrile yields Li_2TCNQF_4. However, deviation from this ratio or the reaction temperature gives either $LiTCNQF_4$ or a mixture of Li_2TCNQF_4 and $LiTCNQF_4$. This is the first report of the large-scale chemical synthesis of Li_2TCNQF_4. Attempts to prepare a single crystal of Li_2TCNQF_4 have been unsuccessful, although air-stable $(Pr_4N)_2TCNQF_4$ was obtained by mixing Pr_4NBr with Li_2TCNQF_4 in aqueous solution. $Pr_4NTCNQF_4$ was also obtained by reaction of $LiTCNQF_4$ with Pr_4NBr in water. Li_2TCNQF_4, $(Pr_4N)_2TCNQF_4$, and $Pr_4NTCNQF_4$ have been characterized by UV−vis, FT-IR, Raman, and NMR spectroscopy, high resolution electrospray ionization mass spectrometry, and electrochemistry. The structures of single crystals of $(Pr_4N)_2TCNQF_4$ and $Pr_4NTCNQF_4$ have been determined by X-ray crystallography. These $TCNQF_4^{2-}$ salts will provide useful precursors for the synthesis of derivatives of the dianions.

1. INTRODUCTION

7,7,8,8-Tetracyanoquinodimethane (TCNQ) has been a molecule of great of interest, as it is a strong electron acceptor.[1,2] However, the tetrafluorinated TCNQ derivative 2,3,5,6-tetrafluoro-7,7,8,8-tetracyanoquinodimethane ($TCNQF_4$) is an even stronger electron acceptor than TCNQ with a higher electron affinity (~3.3 eV[3−5] compared with ~2.9 eV for TCNQ[5,6]). Despite this, to date, $TCNQF_4$-based charge transfer (CT) complexes have been much less studied than their TCNQ counterparts. The radical monoanions of TCNQ and $TCNQF_4$ are stable in air at least for several hours and can be synthesized by chemical or electrochemical reduction of TCNQ or $TCNQF_4$. Thus, metal and organic derivatives based on either $TCNQ^{\bullet-}$ or $TCNQF_4^{\bullet-}$ have been prepared, and their physical properties, such as magnetism,[7−10] electronic conductivity,[3,11−14] and electric switching as bulk materials,[15,16] have been widely studied. In contrast, studies of materials derived from $TCNQ^{2-}$ as well as $TCNQF_4^{2-}$ dianions are limited.

There have been several reports of X-ray crystal structures of $TCNQ^{2-}$-based complexes.[17−24] In comparison, only a few coordination polymers containing $TCNQF_4^{2-}$ have been fully characterized by X-ray crystallography: $Mn_2(TCNQF_4^{2-})(solvent)(TCNQF_4^{\bullet-})_2$[25] and $[(Me_5Cp)_2M]_2TCNQF_4$ (M^{III}: Fe, Co).[26] In these studies, the $TCNQ^{2-}/TCNQF_4^{2-}$ dianions resulted from either disproportionation of LiTCNQ/$LiTCNQF_4$ or direct two-electron reduction of TCNQ/$TCNQF_4$ by reactive metallocenes (Fe and Co). The reason for the disproportionation of $TCNQ^{\bullet-}/TCNQF_4^{\bullet-}$ to dianions of TCNQ/$TCNQF_4$ is not yet fully understood.

In solution, the $TCNQ^{2-}$ dianion is sensitive to air and rapidly decomposes into α,α-dicyano-*p*-toluoyl cyanide ($DCTC^-$).[27,28] As a result, syntheses of complexes based on the $TCNQ^{2-}$ dianion are much more difficult than those for the radical monoanion. However, recently, Robson and co-workers have successfully used the air-stable H_2TCNQ as a starting material to produce both metal- and organic-based $TCNQ^{2-}$ complexes.[21−24] In an organic solution in the presence of a weak base, H_2TCNQ undergoes sequential deprotonations to $TCNQ^{2-}$. The generated dianion then combines with metal or organic cations in situ to form new materials. These metal−$TCNQ^{2-}$-based coordination polymers have an ability to establish 3D networks which intercalate redox-active species into the structural units and which may lead to these solid materials having interesting electronic and magnetic properties.[24] Although the $TCNQ^{2-}$ complexes also have attractive

Received: July 23, 2012
Published: November 15, 2012

   dx.doi.org/10.1021/jo301403v | J. Org. Chem. 2012, 77, 10568−10574

Scheme 1. Summary of Reaction Pathways Used for Synthesis of Li_2TCNQF_4, $LiTCNQF_4$, $(Pr_4N)_2TCNQF_4$, and $Pr_4NTCNQF_4$[a]

$$3LiI + TCNQF_4 \xrightarrow[\text{Boiling } CH_3CN]{\text{Pathway 1}} Li_2TCNQF_4 + LiI_3 \quad [1]^*$$
90%

$$3LiI + 2TCNQF_4 \xrightarrow[\text{Cold } CH_3CN]{\text{Pathway 2}} 2LiTCNQF_4 + LiI_3 \quad [2]$$
84%

$$Li_2TCNQF_4 + 2Pr_4NBr \xrightarrow[\text{Hot } H_2O]{\text{Pathway 3}} (Pr_4N)_2TCNQF_4 + 2LiBr \quad [3]$$
95%

$$LiTCNQF_4 + Pr_4NBr \xrightarrow[\text{Hot } H_2O]{\text{Pathway 4}} Pr_4NTCNQF_4 + LiBr \quad [4]$$
68%

[a]*In practice, 4 mol equiv of LiI is needed to obtain complete conversion to Li_2TCNQF_4 due to the I_3^-/I_2 equilibrium.

features, they differ significantly from the better known $TCNQ^{\bullet-}$-based materials. For example, $TCNQ^{2-}$ can bind strongly to the metal ion[21,23] and is free from $\pi-\pi$ contacts.[23,24] Consequently, new types of coordination polymers can be formed with intercalation of oxidants or reductants into the structure, which may change the electric conductivity of these materials.[21,23] Here, we report the one step, direct chemical synthesis as well as the characterization and stability of two new complexes based on the $TCNQF_4^{2-}$ dianion, i.e., Li_2TCNQF_4, $(Pr_4N)_2TCNQF_4$, which can be used as starting reagents to synthesize both metal– and organic–$TCNQF_4^{2-}$-based materials. To the best our knowledge, this is the first report of the chemical synthesis, with a high yield of Li_2TCNQF_4 and $(Pr_4N)_2TCNQF_4$. In addition, single crystals of both $(Pr_4N)_2TCNQF_4$ and the radical monoanion derivative $Pr_4NTCNQF_4$ were structurally characterized by X-ray diffraction methods.

2. RESULTS AND DISCUSSION

2.1. Synthesis. As noted already, $LiTCNQF_4$ is an important starting reagent for the synthesis of $TCNQF_4^{\bullet-}$-based materials. Our initial attempts to synthesize $LiTCNQF_4$ was based on the literature procedure described for the preparation of LiTCNQ.[2] However, it was found that these reaction conditions produced a mixture of $LiTCNQF_4$ and Li_2TCNQF_4 as proved by UV–vis spectroscopy and electrochemistry (see below). Subsequently, it was shown that the synthetic conditions could be optimized to favor the formation of Li_2TCNQF_4, which can be an important starting salt for the synthesis of $TCNQF_4^{2-}$ dianion coordination polymers. This optimization study has demonstrated that the ratio of Li_2TCNQF_4 and $LiTCNQF_4$ generated depends on the reaction temperature, duration of the reaction, and the molar ratio of the reactants used in the synthesis.

A straightforward method for the synthesis of Li_2TCNQF_4 is summarized in pathway 1 (Scheme 1) as the overall balanced equation. However, in practice, 4 mol equiv of LiI is needed for complete conversion to Li_2TCNQF_4. Without an excess LiI, a small amount of $LiTCNQF_4$ is obtained. Thus, a boiling solution of LiI (273 mg, 2.04 mmol) in acetonitrile (15 mL) was added dropwise to a boiling solution of $TCNQF_4$ (142 mg, 0.51 mmol) in acetonitrile (15 mL). The resulting mixture was stirred for 1 h at 50–60 °C under N_2. The suspension was cooled to room temperature before filtration to collect the solid. The crude product was washed with diethyl ether (dried and degassed prior to use) until no triiodide was detected in the solution. A creamy white solid (134 mg, 90%) was obtained after drying under vacuum over P_2O_5 for 3 h. The solid was then characterized using FT-IR, Raman, and UV–vis spectroscopy and electrochemistry (see below). These data indicate that Li_2TCNQF_4 is free of $LiTCNQF_4$. High resolution electrospray ionization mass spectrometry (ESI-MS) also confirms that the charge on the $TCNQF_4$ moiety is −2 (calculated for $C_{12}F_4N_4^{2-}$: m/z 138.0030 (100%); found: m/z 138.0026 (100%)). The elemental analysis is consistent with the formula $Li_2TCNQF_4 \cdot H_2O$; however, as seen later, there is no water detected in the infrared spectrum. Li_2TCNQF_4 is unstable in air, even in the solid state, and over time is gradually converted to $LiTCNQF_4$ (see Figure S1, Supporting Information). Efforts to grow a single crystal of Li_2TCNQF_4 have proved unsuccessful. The same reaction conditions, but using a 3:1 molar ratio of LiI and $TCNQF_4$, yielded a mixture of Li_2TCNQF_4 and $LiTCNQF_4$. The mixture was quantitatively analyzed using UV–vis spectroscopy and electrochemistry as described in Supporting Information. Li_2TCNQF_4 was found to be produced under these conditions at a level of 90–95% (molar %) with the remainder of the sample being $LiTCNQF_4$ (Figures S2 and S3, Supporting Information).

To favor the reduction of $TCNQF_4$ to $TCNQF_4^{\bullet-}$ rather than to $TCNQF_4^{2-}$, the reaction conditions used for the synthesis of Li_2TCNQF_4 needed to be modified. Thus, the molar ratio of LiI and $TCNQF_4$ was changed to 3:2, and the reaction was carried out with cold solutions (pathway 2, Scheme 1). Three milliliters of a cold (0 °C) acetonitrile solution containing LiI (75.4 mg, 0.57 mmol) was added dropwise into 8 mL of a cold acetonitrile solution of $TCNQF_4$ (104 mg, 0.38 mmol). The resulting mixture was placed in an ice bath and stirred under N_2 for 30 min. The precipitate that formed was isolated rapidly by vacuum filtration, followed by washing with acetonitrile (3 × 3 mL) and diethyl ether (3 × 5 mL), and dried over P_2O_5 under vacuum overnight. The purple solid obtained (89.5 mg, 84%) was studied using a wide range of spectroscopic techniques and electrochemistry. These data (see below) confirmed that $LiTCNQF_4$ was the only product produced in

dx.doi.org/10.1021/jo301403v | J. Org. Chem. 2012, 77, 10568–10574

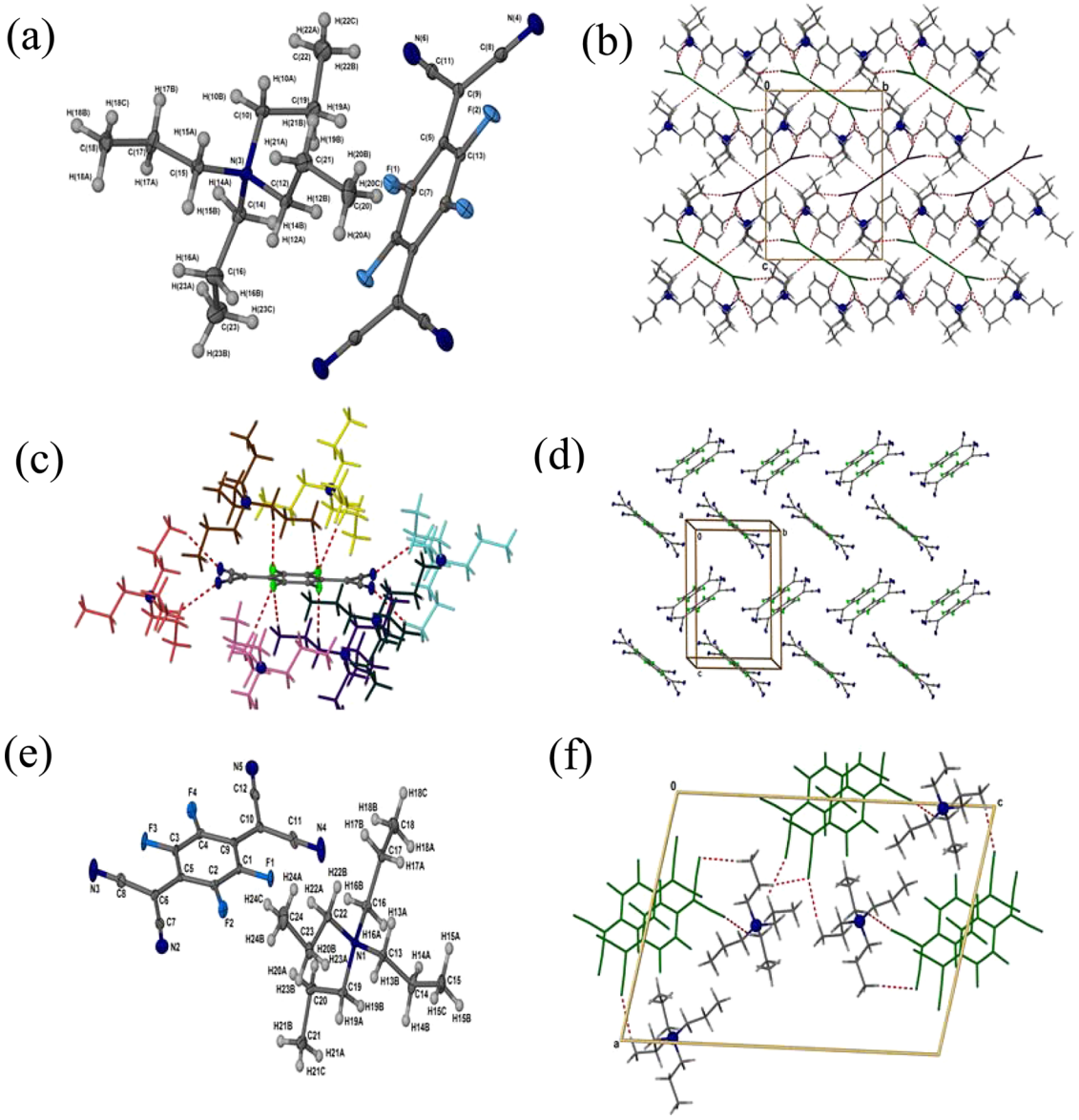

Figure 1. X-ray single crystal structures: (a) asymmetric unit of $(Pr_4N)_2TCNQF_4$; (b) packing diagram of $(Pr_4N)_2TCNQF_4$ viewed along the *a* axis; (c) hydrogen-bonding interactions in $(Pr_4N)_2TCNQF_4$; (d) packing diagram of $TCNQF_4^{2-}$ anions in $(Pr_4N)_2TCNQF_4$; (e) the asymmetric unit of $Pr_4NTCNQF_4$; (f) the packing diagram of $Pr_4NTCNQF_4$ viewed along the *b* axis.

Table 1. Some Examples of Intramolecular Bond Distances Reported for $TCNQF_4$, $TCNQF_4^{\bullet-}$, and $TCNQF_4^{2-}$

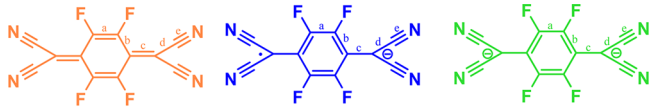

$TCNQF_4$ $TCNQF_4^{\bullet-}$ $TCNQF_4^{2-}$

	a/Å	*b*/Å	*c*/Å	*d*/Å	*e*/Å	ρ	ref
$TCNQF_4^0$	1.334	1.437	1.372	1.437	1.140	0.00	26
$(n\text{-}Bu_4N)TCNQF_4$	1.360	1.420	1.429	1.435	1.140	−1.00	30
$Pr_4NTCNQF_4$	1.357	1.419	1.415	1.424	1.152	−0.94	this work
$[(Me_5Cp)_2Fe]_2TCNQF_4$	1.373	1.398	1.457	1.403	1.154	−2.00	26
$(Pr_4N)_2TCNQF_4$	1.377	1.403	1.456	1.406	1.161	−1.92	this work

pathway 2. Clearly, the reduction of $TCNQF_4$ is thermodynamically controlled, so an excess of LiI gives rise to the further reduction of $TCNQF_4^{\bullet-}$ to $TCNQF_4^{2-}$ as illustrated in pathway 1 of Scheme 1.

Both Li_2TCNQF_4 and $LiTCNQF_4$ directly reacted with Pr_4NBr in water (pathways 3 and 4, Scheme 1) to yield colorless solids of $(Pr_4N)_2TCNQF_4$ and a blue powder for $Pr_4NTCNQF_4$. Single crystals of $(Pr_4N)_2TCNQF_4$ and

dx.doi.org/10.1021/jo301403v | J. Org. Chem. 2012, 77, 10568−10574

$Pr_4NTCNQF_4$ suitable for X-ray crystallographic analysis were obtained by either diffusion of *n*-pentane into an acetone solution of $(Pr_4N)_2TCNQF_4$ or diffusion of diethyl ether into a methanol solution of $Pr_4NTCNQF_4$. The polycrystalline solids of both $(Pr_4N)_2TCNQF_4$ and $Pr_4NTCNQF_4$ are stable in air and characterized by ^{19}F NMR, FT-IR, Raman, and UV−vis spectroscopy and electrochemistry. All spectroscopic data are consistent with the single crystal structures.

2.2. X-ray Structural Characterization of $(Pr_4N)_2TCNQF_4$ and $Pr_4NTCNQF_4$. Colorless diamond-like $(Pr_4N)_2TCNQF_4$ crystallized in the monoclinic space group $P2_1/n$. The asymmetric unit contains one Pr_4N^+ cation and a half $TCNQF_4^{2-}$ anion. Figure 1a shows the cation and the whole anion positions in this structure. The structure of $(Pr_4N)_2TCNQF_4$ is composed of a 3D layered network supported by hydrogen bonding (Figure 1b). The charge (ρ) on the $TCNQF_4$ moieties in $(Pr_4N)_2TCNQF_4$ has been estimated by the mean bond lengths of $TCNQF_4$ (Table 1) using the Kistenmacher relationship, $\rho = A[c/(b + d)] + B$ (A = −46.729 and B = 22.308). A and B were determined from neutral $TCNQF_4$ (ρ = 0)[29] and $TCNQF_4^{\bullet-}$ monoanion in *n*-$Bu_4NTCNQF_4$ (ρ = −1).[30] The calculated ρ value (−1.92) supports the assignment of $TCNQF_4^{2-}$ dianions. Moreover, the structural parameters in $(Pr_4N)_2TCNQF_4$ are consistent with those for $TCNQF_4^{2-}$ species reported by Miller et al.[26] (Table 1). The $TCNQF_4$ moieties in $(Pr_4N)_2TCNQF_4$ are not planar because the C(CN) groups lie away from the phenyl plane with a diangle of 17°. Each $TCNQF_4$ moiety interacts with seven Pr_4N^+ cations via hydrogen bond interactions between the CN/F groups of the $TCNQF_4$ moieties and the CH groups from the Pr_4N^+ cations (Figure 1c; Table S1, Supporting Information). Moreover, the adjacent $TCNQF_4^{2-}$ layers are separated by Pr_4N^+ cation layers and oriented with an angle between the respective phenyl planes of about 59.2° (Figure 1d). In addition, the Pr_4N^+ cations and the $TCNQF_4^{2-}$ anions are connected by hydrogen bonding to form a 3D network (Figure 1b; Table S1, Supporting Information).

Dark-blue needles of $Pr_4NTCNQF_4$ crystallize in the monoclinic space group $P2_1/n$, and the 3D H-bonded network structure consists of $(TCNQF_4^{\bullet-})_2$ dimers and Pr_4N^+ cations (Figure 1f; Table S2, Supporting Information). The asymmetric unit of $Pr_4NTCNQF_4$ is shown in Figure 1e. Each $TCNQF_4$ anion is almost planar with a slight bowing of the C≡N groups away from the phenyl plane. The two neighboring $TCNQF_4^{\bullet-}$ anions eclipse to form a face-to-face π-stacked dimer with an interplanar distance of 3.147 Å, a remarkably short spacing compared with that of normal $\pi-\pi$ stacked TCNQ or $TCNQF_4$ dimers (ca. 3.30 Å).[7,8,11,30] The overlap of the dimer is ring over bond mode. The degree of charge transfer of $TCNQF_4$ species in $Pr_4NTCNQF_4$ has been determined using the same method applied to $(Pr_4N)_2TCNQF_4$ and found to be −0.94. Therefore, the $TCNQF_4$ moieties in $Pr_4NTCNQF_4$ can be described as the $TCNQF_4^{\bullet-}$ radical monoanion. The structural parameters for $Pr_4NTCNQF_4$ also agree well with those expected for $TCNQF_4^{\bullet-}$ (Table 1) and found in related complexes reported by us and others.[7,8,30,32,34]

2.3. FT-IR and Raman Spectroscopy. Infrared and Raman spectroscopy have been used widely to determine the redox state of $TCNQF_4$ in previously synthesized materials.[25,31,32] The IR bands in the solid state are shown in Table 2 and compared with the neutral $TCNQF_4$. The C≡N stretch is diagnostic and shifts to lower energy with the increased state of reduction.[7,26,30,32−34] The C−F out-of-plane bending mode is also sensitive to the increased charge on the $TCNQF_4$ moiety, shifting to higher energies across the series $TCNQF_4^0$ → $TCNQF_4^{\bullet-}$ → $TCNQF_4^{2-}$ as shown in Table 2.

Table 2. Some Characteristic FT-IR Bands for $TCNQF_4$, $LiTCNQF_4$, Li_2TCNQF_4, $(Pr_4N)_2TCNQF_4$, and $Pr_4NTCNQF_4$

compound	ν(C≡N)/cm^{-1}	δ(C−F)/cm^{-1}
$TCNQF_4$	2228	1192
$LiTCNQF_4$	2219, 2188	1204
$Pr_4NTCNQF_4$	2200, 2182	1204
Li_2TCNQF_4	2184, 2151, 2125	1250
$(Pr_4N)_2TCNQF_4$	2164, 2130, 2092	1222

The Raman spectrum of the neutral $TCNQF_4$ (Figure S2, Supporting Information) is dominated by three bands at 2226, 1665, and 1457 cm^{-1} which respectively correspond to C≡N, C=C ring, C−CN wing stretches.[3,31] These Raman vibration modes exhibit shifts consistent with reduced $TCNQF_4^{\bullet-}$ (Figure 2a,b) and $TCNQF_4^{2-}$(Figure 2c,d), respectively.

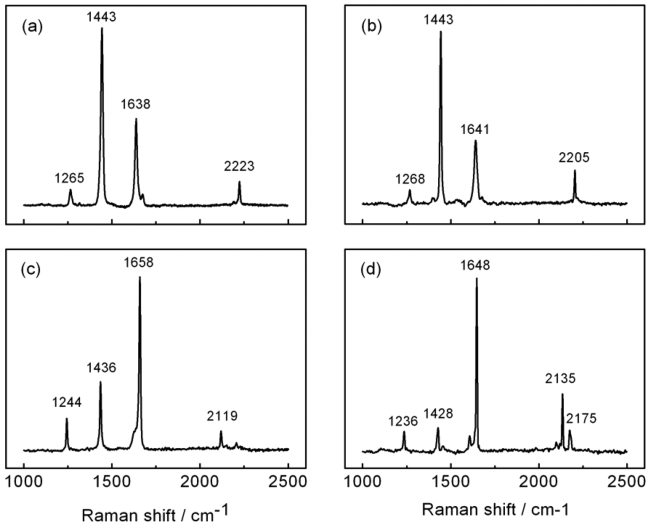

Figure 2. Raman spectra of solid samples of (a) $LiTCNQF_4$, (b) $Pr_4NTCNQF_4$, (c) Li_2TCNQF_4, and (d) $(Pr_4N)_2TCNQF_4$.

2.4. Characterization in Solution. UV−vis spectra for $LiTCNQF_4$, $Pr_4NTCNQF_4$, Li_2TCNQF_4, and $(Pr_4N)_2TCNQF_4$ dissolved in acetonitrile are shown in Figure 3. These spectra are dominated by two intense charge transfer bands with λ_{max} at 411 and 752 nm for the $LiTCNQF_4$ and $Pr_4NTCNQF_4$ salts which are characteristic of the $TCNQF_4^{\bullet-}$.[4] The dissolved Li_2TCNQF_4 and $(Pr_4N)_2TCNQF_4$ salts also exhibit two intense absorption bands with λ_{max} at 333 and 218 nm assigned to the $TCNQF_4^{2-}$ dianion.[4] The molar extinction coefficients (ε) at 411 nm ($TCNQF_4^{\bullet-}$) and at 333 nm ($TCNQF_4^{2-}$) were calculated using electrochemically reduced samples, $\varepsilon_{(\lambda_{max}\ 411\ nm)} = 5.08 \pm 0.17 \times 10^4$ M^{-1} cm^{-1} and $\varepsilon_{(\lambda_{max}\ 333\ nm)} = 4.06 \pm 0.17 \times 10^4$ M^{-1} cm^{-1} and these values were used to determine the concentrations for the $LiTCNQF_4$, $Pr_4NTCNQF_4$, Li_2TCNQF_4, and $(Pr_4N)_2TCNQF_4$ solutions.

^{19}F NMR spectroscopy was also used to investigate these salts in methanol-d_4. The ^{19}F NMR spectrum for $(Pr_4N)_2TCNQF_4$ in methanol-d_4 gives rise to a sharp singlet at −147.52 ppm (Figure 4a) indicating only the diamagnetic $TCNQF_4^{2-}$ species present in solution. However, as expected, both paramagnetic

dx.doi.org/10.1021/jo301403v | J. Org. Chem. 2012, 77, 10568−10574

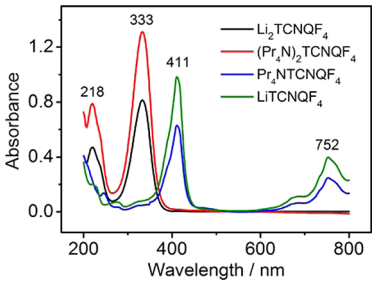

Figure 3. UV−vis spectra for $LiTCNQF_4$, 0.018 mM; $Pr_4NTCNQF_4$, 0.012 mM; Li_2TCNQF_4, 0.02 mM; $(Pr_4N)_2TCNQF_4$, 0.033 mM in acetonitrile. The concentrations were calculated using $\varepsilon_{(\lambda_{max}\text{ at }411\text{ nm})} = 5.08 \pm 0.17 \times 10^4\ M^{-1}\ cm^{-1}$ for $TCNQF_4^{\bullet-}$ and $\varepsilon_{(\lambda_{max}\text{ at }333\text{ nm})} = 4.06 \pm 0.17 \times 10^4\ M^{-1}\ cm^{-1}$ for $TCNQF_4^{2-}$.

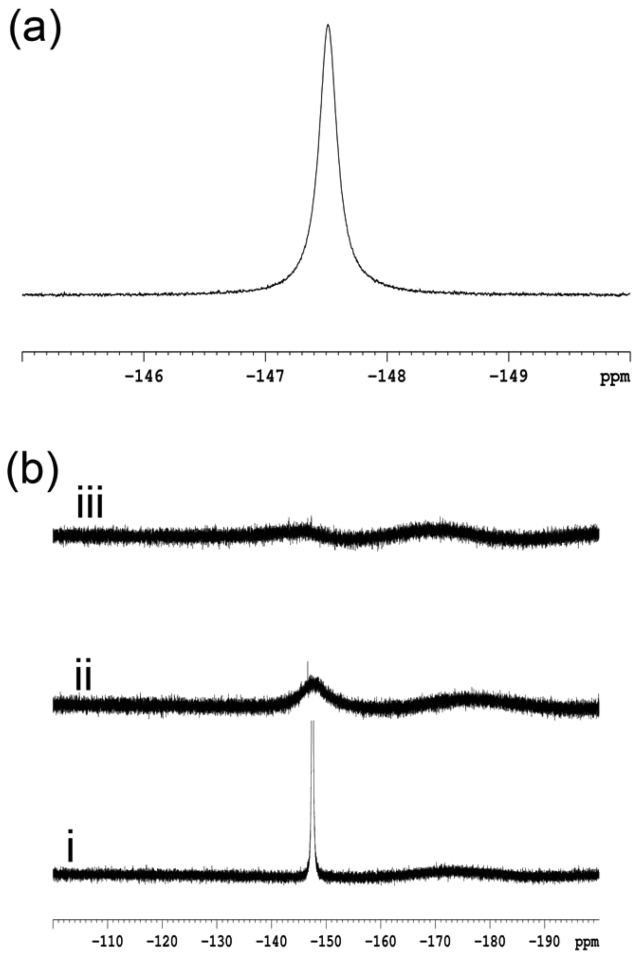

Figure 4. ^{19}F NMR spectra in methanol-d_4. (a) $(Pr_4N)_2TCNQF_4$, (b) (i) 34.5 mM $(Pr_4N)_2TCNQF_4$, (ii) 34.5 mM $(Pr_4N)_2TCNQF_4$ + 0.086 mM $Pr_4NTCNQF_4$, (iii) 34.5 mM $(Pr_4N)_2TCNQF_4$ + 0.17 mM $Pr_4NTCNQF_4$.

$TCNQF_4^{\bullet-}$ salts show no clear resonances. To ascertain the effect of small amounts of the paramagnetic $TCNQF_4^{\bullet-}$ on the spectrum of the diamagnetic $(Pr_4N)_2TCNQF_4$ salt, a solution of $Pr_4NTCNQF_4$ was titrated into the diamagnetic $(Pr_4N)_2TCNQF_4$, Figure 4b. The original sharp singlet from $(Pr_4N)_2TCNQF_4$ (Figure 4b(i)) is immediately broadened by addition of only 0.25% mol equiv (Figure 4b(ii)), whereas addition of 0.5% almost completely removed any signals (Figure 4b(iii)). This extreme sensitivity to traces of paramagnetic material supports the high purity of the $(Pr_4N)_2TCNQF_4$ in terms of possible contamination by $TCNQF_4^{\bullet-}$. Note that electron self-exchange between the $TCNQF_4^{\bullet-}$ and $TCNQF_4^{2-}$ species is likely to contribute to the line broadening when a mixtures of these two species are present. Also, it was not surprising that despite our best attempts to obtain the ^{19}F NMR spectrum for Li_2TCNQF_4, using drybox conditions and various solvents (e.g., MeCN-d_3 or MeOH-d_4), only a complicated pattern of paramagnetically broadened, weak signals were observed (data not shown).

Steady-state voltammetry also was used to determine the redox levels of $TCNQF_4$ in the synthesized materials. Figure 6a shows nearly a steady-state voltammogram for an acetonitrile (0.1 M Bu_4NPF_6) solution containing the product formed via pathway 1 (Scheme 1). Clearly, the product obtained in boiling acetonitrile with a 4:1 molar ratio of LiI and $TCNQF_4$ contains only $TCNQF_4^{2-}$, devoid of $TCNQF_4^{\bullet-}$, as only oxidation current associated with the $TCNQF_4^{2-/\bullet-}$ and $TCNQF_4^{\bullet-/0}$ processes are detected. Figure 6b shows the near steady-state voltammogram in acetonitrile (0.1 M Bu_4NPF_6) after dissolution of $LiTCNQF_4$ solid, synthesized via pathway 2. In this case, only $TCNQF_4^{\bullet-}$ is present as the zero current position lies midway between the currents for the $TCNQF_4^{\bullet-/2-}$ reduction and the $TCNQF_4^{\bullet-/0}$ oxidation processes. The same steady-state voltammetric behavior is observed for the product formed via pathway 4 (Figure S4, Supporting Information), confirming that only the $TCNQF_4^{\bullet-}$ species and no $TCNQF_4^{2-}$ is present in the original solid $Pr_4NTCNQF_4$. The near steady-state voltammogram for $(Pr_4N)_2TCNQF_4$ (Figure 6c) in acetonitrile (0.1 M Bu_4NPF_6) is similar to that for Li_2TCNQF_4. The result implies that only $TCNQF_4^{2-}$ is present in this synthesized solid.

3. CONCLUSION

The reduction of $TCNQF_4$ by iodide is a thermodynamically controlled process. Hence, either $LiTCNQF_4$ or Li_2TCNQF_4 can be generated by controlling the reaction temperature and the molar ratio of the reaction of $TCNQF_4$ with LiI. This appears to be the first report of the chemical synthesis of Li_2TCNQF_4 in high yield. Li_2TCNQF_4 is slowly oxidized to $LiTCNQF_4$ in air. However, $(Pr_4N)_2TCNQF_4$ is stable in air and is recommended as a synthetic precursor for the synthesis of a range of materials based on $TCNQF_4^{2-}$. The X-ray structural analysis of single crystals of both $(Pr_4N)_2TCNQF_4$ and $Pr_4NTCNQF_4$ shows the presence of 3D H-supported networks. Electrochemical data, Raman, FT-IR, and UV−vis spectra, and elemental analysis are all consistent with the formulations derived from the crystal structures of $(Pr_4N)_2TCNQF_4$ and $Pr_4NTCNQF_4$. ^{19}F NMR spectra obtained from the pure $(Pr_4N)_2TCNQF_4$ and titration with $Pr_4NTCNQF_4$ in $(Pr_4N)_2TCNQF_4$ confirmed that $TCNQF_4^{2-}$ is diamagnetic and that the paramagnetic $TCNQF_4^{\bullet-}$ broadens the resonances.

4. EXPERIMENTAL SECTION

4.1. Chemicals. Tetrapropylammonium bromide, lithium iodide, *n*-pentane, methanol, acetone, and $TCNQF_4$ were used as received. Acetonitrile and diethyl ether were dried before use. Bu_4NPF_6 was recrystallized twice from ethanol. All aqueous solutions were prepared from high purity water (resistivity of 18.2 MΩ·cm). All synthetic reactions were performed under N_2 using standard Schlenk techniques.

4.2. Synthesis of Li_2TCNQF_4. A boiling solution of LiI (273 mg, 2.04 mmol) in acetonitrile (15 mL) was added dropwise to a boiling

dx.doi.org/10.1021/jo301403v | J. Org. Chem. 2012, 77, 10568−10574

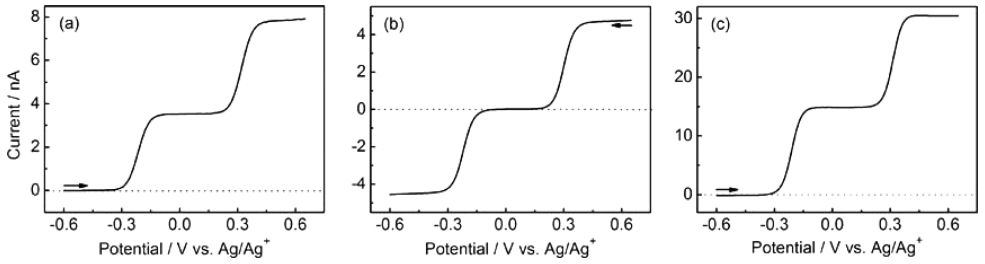

Figure 6. Near steady-state voltammograms of (a) 1.0 mM Li_2TCNQF_4, (b) 1.0 mM $LiTCNQF_4$, and (c) 4.5 mM $(Pr_4N)_2TCNQF_4$ in acetonitrile (0.1 M Bu_4NPF_6) obtained with a 12.0 μm diameter carbon fiber microelectrode at a scan rate of 20 mV s^{-1}.

solution of $TCNQF_4$ (142 mg, 0.51 mmol) in acetonitrile (15 mL). The resulting mixture was stirred for 1 h at 50−60 °C under N_2. The suspension was cooled to room temperature before filtration to collect the solid. The crude product was washed with diethyl ether (dried and degassed prior use) until no LiI_3 was detected in the solution. Thus, pure Li_2TCNQF_4, was obtained as a creamy white solid as after drying under vacuum for 3 h (134 mg, 90%). FT-IR (ν/cm^{-1}): CN: 2184 (s), 2151 (s) 2125 (s). UV−vis (λ_{max} nm): 333 ($TCNQF_4^{2-}$), 218 ($TCNQF_4^{2-}$). HRMS: Calcd for $(C_{12}F_4N_4)^{2-}$ m/z 138.0030; found: m/z 138.0026 (100%). Anal. Calcd. for $Li_2TCNQF_4{\cdot}H_2O$ [$Li_2C_{12}F_4N_4H_2O$]: C, 46.79, H 0.65, N, 18.19. Found: C 46.29, H 0.86, N 18.34%.

4.3. Synthesis of $LiTCNQF_4$ (pathway 2, Scheme 1). Three milliliters of a cold (0 °C) acetonitrile solution containing LiI (75.4 mg, 0.57 mmol) was added dropwise into 8 mL of a cold acetonitrile solution of $TCNQF_4$ (104 mg, 0.38 mmol). The resulting mixture was placed in an ice bath and stirred under N_2 for 30 min. The precipitate that formed was isolated rapidly by vacuum filtration, followed by washing with acetonitrile (3 × 3 mL) and diethyl ether (3 × 5 mL), and dried over P_2O_5 under vacuum overnight. A purple solid was obtained (89.5 mg, 84%). FT-IR (ν/cm^{-1}): 2219 (m), 2188 (s), 1625 (m), 1532 (s), 1501 (m), 1351 (s), 1204 (m), 967 (s). High resolution MS: Calcd for $(C_{12}F_4N_4)^{\bullet-}$ m/z 276.0059; found: m/z 276.0140 (100%). UV−vis (λ_{max} nm): 752 ($TCNQF_4^{\bullet-}$), 411 ($TCNQF_4^{\bullet-}$).

4.4. Synthesis of $(Pr_4N)_2TCNQF_4$ (pathway 3, Scheme 1). Pr_4NBr (84.8 mg, 0.32 mmol) was dissolved in hot water (5 mL, degassed) and added to an aqueous solution of Li_2TCNQF_4 (30 mg, 0.11 mmol, in 5 mL of degassed hot water). The white precipitate that formed immediately was filtered, washed with hot water (3 × 10 mL) and diethyl ether (3 × 15 mL), and dried over P_2O_5 under vacuum overnight (62.5 mg, 93%). Colorless single crystals of $(Pr_4N)_2(TCNQF_4)$ suitable for X-ray crystallographic analysis were obtained by diffusion of n-pentane into a n-acetone solution of $(Pr_4N)_2TCNQF_4$ over 5 days. ^{19}F NMR (376 MHz, δ/ppm, methanol-d_4): −147.52 (s). FT-IR (ν/cm^{-1}): 2979 (w), 2949(w), 2885 (w), 2164 (s, CN), 2130 (s, CN), 2092 (w, CN) 1475 (s), 1222 (m), 1133 (m), 986 (w), 958 (m), 781 (m), 760 (w), 750 (w). UV−vis (nm): 333 ($TCNQF_4^{2-}$), 218 ($TCNQF_4^{2-}$). Anal. Calcd for $(Pr_4N)_2TCNQF_4$ [$C_{36}H_{56}F_4N_6$]: C 66.64, H 8.70, N 12.95%. Found: C 66.49, H 9.01, N 13.31%.

4.5. Synthesis of $Pr_4NTCNQF_4$, (pathway 4, Scheme 1). Five milliliters of a hot aqueous solution of Pr_4NBr (51.7 mg, 0.19 mmol) was added into 5 mL of a hot aqueous solution of $LiTCNQF_4$ (50 mg, 0.18 mmol). The dark blue solid that formed immediately was filtered, washed with hot water (3 × 15 mL) and diethyl ether (3 × 15 mL), and then dried over P_2O_5 under vacuum overnight (43 mg, 68%). Dark-blue needle crystals of $Pr_4NTCNQF_4$ suitable for X-ray crystallography were obtained by diffusion of diethyl ether into a methanol solution of $Pr_4NTCNQF_4$ over a week. FT-IR (ν/cm^{-1}): 2975 (w) 2943 (w), 2881 (w), 2200 (s, CN), 2182 (s, CN), 1633 (w), 1603 (w), 1536 (m), 1502 (w), 1472(w), 1390 (s), 1347 (m), 1337 (m), 1204(w), 1142 (w), 967 (s), 872 (w), 756 (w). UV−vis (nm): 752 ($TCNQF_4^{\bullet-}$), 411 ($TCNQF_4^{\bullet-}$). Anal. Calcd for $P_4NTCNQF_4$, [$C_{24}H_{28}F_4N_5$]: C, 62.32, H 6.10, N, 15.14%. Found: C, 62.49, H 6.25, N, 15.31%.

4.6. Electrochemical Procedures and Instrumentation. Voltammetric experiments under near steady-state conditions were conducted in acetonitrile (0.1 M Bu_4NPF_6) with an electrochemical workstation using a standard three-electrode cell configuration at room temperature (22 ± 2 °C). The working electrode (WE) was calibrated to be a 12.0 μm diameter carbon fiber microelectrode (diameter is 11 ± 2 μm). A platinum wire was used as the counter electrode. A silver wire immersed in acetonitrile solution containing 1.0 mM $AgNO_3$ and 0.1 M Bu_4NPF_6 was used as a Ag/Ag^+ reference electrode (RE) (the potential is −135 ± 5 mV versus the ferrocene/ferrocenium couple $Fc^{0/+}$). The RE was separated from the test solution by a salt bridge containing the relevant supporting electrolyte.

4.7. Physical Characterization Procedures. FT-IR spectra were recorded using an ATR instrument using the neat solids. Raman spectra were acquired from the neat solid with a spectrometer and microscope using 633 nm laser line. ^{19}F NMR spectra were recorded using a 400/300 MHz spectrometer at 376/282 MHz with chemical shifts reported relative to an external reference of $CFCl_3$ at 0.00 ppm. Mass spectra were acquired on an electrospray ionization mass spectrometer by direct infusion using a syringe pump, and the spectra were run in positive ion mode. X-ray structural data were collected at the Australian Synchrotron using the PX1 beamline operating at 15 keV (λ = 0.7292 Å). The collection temperature was maintained at 100 K using an open-flow N_2 cryostream. Initial data processing was carried out using XDS software.[35] Both structures were solved by direct methods using SHELXS-97.[36] Least-squares refinements against F2 were carried out using SHELXL-97, with the program X-Seed as a graphical interface.[37] All hydrogen atoms were placed in idealized positions and refined using a riding model. Documentations CCDC-831469 (for $(Pr_4N)_2TCNQF_4$) and -831468 (for $Pr_4NTCNQF_4$) contain the supplementary crystallographic data obtained for this report. These data can be obtained free of charge from The Cambridge Crystallographic Data Centre via www.ccdc.cam.ac.uk/data_request/cif.

■ ASSOCIATED CONTENT

Supporting Information

Figure S1: Stability of Li_2TCNQF_4; Figure S2: UV−vis study of a mixture of Li_2TCNQF_4 and $LiTCNQF_4$; Figure S3: electrochemical study of a mixture of Li_2TCNQF_4 and $LiTCNQF_4$; Figure S4: electrochemistry of $Pr_4NTCNQF_4$; Figure S5: Raman spectrum of neutral $TCNQF_4$. Tables S1 and S2 contain additional crystallographic information for $(Pr_4N)_2TCNQF_4$ and $Pr_4NTCNQF_4$. This material is available free of charge via the Internet at http://pubs.acs.org.

■ AUTHOR INFORMATION

Corresponding Author

*E-mail: Alan.Bond@monash.edu; Lisa.Martin@monash.edu.

Notes

The authors declare no competing financial interest.

■ ACKNOWLEDGMENTS

Financial support from the Australian Research Council (ARC) to A.M.B. and L.L.M. is gratefully acknowledged. T.H.L. is very appreciative of a graduate scholarship from Danang City in

Vietnam and a stipend provided by the Monash University, Faculty of Science Dean's International Postgraduate Research Scholarship. D.A.K.T. thanks the ARC Super Science Fellowship. The authors also thank Professor Don McNaughton for helpful discussions. Finally, we acknowledge the Australian Synchrotron for beam-time.

REFERENCES

(1) Acker, D. S.; Harder, R. J.; Hertler, W. R.; Mahler, W.; Melby, L. R.; Benson, R. E.; Mochel, W. E. *J. Am. Chem. Soc.* **1960**, *82*, 6408−6409.
(2) Melby, L. R.; Mahler, W.; Mochel, W. E.; Harder, R. J.; Hertler, W. R.; Benson, R. E. *J. Am. Chem. Soc.* **1962**, *84*, 3374−3387.
(3) Xiao, K.; Rondinone, A. J.; Puretzky, A. A.; Ivanov, I. N.; Retterer, S. T.; Geohegan, D. B. *Chem. Mater.* **2009**, *21*, 4275−4281.
(4) Le, T. H.; Nafady, A.; Qu, X.; Martin, L. L.; Bond, A. M. *Anal. Chem.* **2011**, *83*, 6731−6737.
(5) Sobczyk, M.; Skurski, P.; Simons, J. *J. Phys. Chem. A* **2003**, *107*, 7084−7091.
(6) Jerome, D. *Chem. Rev.* **2004**, *104*, 5565−5591.
(7) Lopez, N.; Zhao, H. H.; Prosvirin, A. V.; Wernsdorfer, W.; Dunbar, K. R. *Dalton Trans.* **2010**, *39*, 4341−4352.
(8) Lopez, N.; Prosvirin, A. V.; Zhao, H. H.; Wernsdorfer, W.; Dunbar, K. R. *Chem.—Eur. J.* **2009**, *15*, 11390−11400.
(9) Jain, R.; Kabir, K.; Gilroy, J. B.; Mitchell, K. A. R.; Wong, K. C.; Hicks, R. G. *Nature* **2007**, *445*, 291−294.
(10) Nakamura, Y.; Iwamura, H. *Bull. Chem. Soc. Jpn.* **1993**, *66*, 3724−3728.
(11) Qu, X. H.; Lu, J. Z.; Zhao, C. A.; Boas, J. F.; Moubaraki, B.; Murray, K. S.; Siriwardana, A.; Bond, A. M.; Martin, L. L. *Angew. Chem., Int. Ed.* **2011**, *50*, 1589−1592.
(12) Ishiguro, T.; Yamaji, K.; Saito, G. *Organic Superconductors*, 2nd ed.; Springer-Verlag: New York, 1998.
(13) Chen, W.; Chen, S.; Qi, D. C.; Gao, X. Y.; Wee, A. T. S. *J. Am. Chem. Soc.* **2007**, *129*, 10418−10422.
(14) Yan, J. M. *Solid State Commun.* **1992**, *84*, 895−899.
(15) Potember, R. S.; Poehler, T. O.; Rappa, A.; Cowan, D. O.; Bloch, A. N. *Synth. Met.* **1982**, *4*, 371−380.
(16) Kotsiliou, A. M.; Risen, W. M. *Solid State Commun.* **1988**, *68*, 503−505.
(17) Shimomura, S.; Matsuda, R.; Tsujino, T.; Kawamura, T.; Kitagawa, S. *J. Am. Chem. Soc.* **2006**, *128*, 16416−16417.
(18) Miller, J. S.; Zhang, J. H.; Reiff, W. M.; Dixon, D. A.; Preston, L. D.; Reis, A. H.; Gebert, E.; Extine, M.; Troup, J.; Epstein, A. J.; Ward, M. D. *J. Phys. Chem.* **1987**, *91*, 4344−4360.
(19) Choukroun, R.; Lorber, C.; de Caro, D.; Vendier, L. *Organometallics* **2006**, *25*, 4243−4246.
(20) Oshio, H.; Ino, E.; Ito, T.; Maeda, Y. *Bull. Chem. Soc. Jpn.* **1995**, *68*, 889−897.
(21) Abrahams, B. F.; Hudson, T. A.; Robson, R. *Cryst. Growth Des.* **2008**, *8*, 1123−1125.
(22) Hudson, T. A.; Robson, R. *Cryst. Growth Des.* **2009**, *9*, 1658−1662.
(23) Abrahams, B. F.; Elliott, R. W.; Hudson, T. A.; Robson, R. *Cryst. Growth Des.* **2010**, *10*, 2860−2862.
(24) Abrahams, B. F.; Elliott, R. W.; Hudson, T. A.; Robson, R. *CrystEngComm* **2012**, *14*, 351−354.
(25) Lopez, N.; Zhao, H. H.; Prosvirin, A. V.; Chouai, A.; Shatruk, M.; Dunbar, K. R. *Chem. Commun.* **2007**, 4611−4613.
(26) Dixon, D. A.; Calabrese, J. C.; Miller, J. S. *J. Phys. Chem.* **1989**, *93*, 2284−2291.
(27) Grossel, M. C.; Duke, A. J.; Hibbert, D. B.; Lewis, I. K.; Seddon, E. A.; Horton, P. N.; Weston, S. C. *Chem. Mater.* **2000**, *12*, 2319−2323.
(28) Suchanski, M. R.; Vanduyne, R. P. *J. Am. Chem. Soc.* **1976**, *98*, 250−252.
(29) Emge, T. J.; Maxfield, M.; Cowan, D. O.; Kistenmacher, T. J. *Mol. Cryst. Liq. Cryst.* **1981**, *65*, 161−178.
(30) O'Kane, S. A.; Clerac, R.; Zhao, H. H.; Xiang, O. Y.; Galan-Mascaros, J. R.; Heintz, R.; Dunbar, K. R. *J. Solid State Chem.* **2000**, *152*, 159−173.
(31) Ouyang, C. B.; Guo, Y. B.; Liu, H. B.; Zhao, Y. J.; Li, G. X.; Li, Y. J.; Song, Y. L.; Li, Y. L. *J. Phys. Chem. C* **2009**, *113*, 7044−7051.
(32) Le, T. H.; Nafady, A.; Lu, J.; Peleckis, G.; Bond, A. M.; Martin, L. L. *Eur. J. Inorg. Chem.* **2012**, 2889−2897.
(33) Wang, X. T.; LiableSands, L. M.; Manson, J. L.; Rheingold, A. L.; Miller, J. S. *Chem. Commun.* **1996**, 1979−1980.
(34) Le, T.; O'Mullane, A.; Martin, L.; Bond, A. *J. Solid State Chem.* **2011**, *15*, 2293−2304.
(35) Kabsch, W. *J. Appl. Crystallogr.* **1993**, *26*, 795−800.
(36) Sheldrick, G. M. *Acta Crystallogr., Sect. A: Found. Crystallogr.* **2008**, *64*, 112−122.
(37) Barbour, L. J. *J. Supramol. Chem.* **2001**, *1*, 189−191.